CHEMISTRY
A EUROPEAN JOURNAL

DOI: 10.1002/chem.200600839

Thermosensitive Copolymer Networks Modify Gold Nanoparticles for Nanocomposite Entrapment

Dongxiang Li,[a] Qiang He,[a, b] Yue Cui,[a] Kewei Wang,[a] Xiaoming Zhang,[a] and Junbai Li*[a]

Abstract: The core-shell gold nanoparticles and copolymer of *N*-isopropylacrylamide (NIPAM) and *N*,*N*′-methylenebisacrylamide (MBAA) hybrids (Au@copolymer) were fabricated through surface-initiated atom-transfer radical polymerization (ATRP) on the surface of gold nanoparticles in 2-propanol/water mixed solvents. The surface of citrate-stabilized gold nanoparticles was first modified by a disulfide initiator for ATRP. The slight cross-linking polymerization between NIPAM and MBAA occurred on the gold surface and resulted in the formation of core-shell Au@copolymer nanostructures that were characterized by TEM, and FTIR and UV-visible spectroscopy. Such synthesized Au@copolymer hybrids possess clearly thermosensitive properties and exhibit "inspire" and "expire" water behavior in response to temperature changes in aqueous solution. Because of this property, we enable to trap and encapsulate smaller nanoparticles by using the free space of the copolymer-network scaffold anchored at the gold surface.

Keywords: copolymerization · encapsulation · gold · nanoparticles · thermosensitivity

Introduction

Much attention has been paid to the modification of gold nanoparticles due to their potential applications in the fields of biology and nanotechnology.[1,2] A number of methods have been developed to decorate gold nanoparticles with various polymer molecules for novel purposes.[3] The polymeric reactions occurring on the surface of gold nanoparticles, such as surface-initiated living cationic polymerization[4] and ring-opening metathesis polymerization,[5] have attracted intense interest. An initiator with a thiol, sulfur, or disulfide group is introduced onto the gold surface through chemical binding. The growth of the polymer chains then progresses along the direction of initiators immobilized on the gold surface to form the core-shell composite. The atom-transfer radical polymerization (ATRP) is becoming a popular method that enables good control of molecular weights and low polydispersity. This living radical polymerization from the surface of micro- or nanoparticle templates can yield core-shell structures based on the "graft-from" strategy.[6] Chains of the well-studied thermosensitive polymer poly(*N*-isopropylacrylamide) (PNIPAM) undergo a thermally induced conformational change from the swelled, hydrophilic state to the shrunken, hydrophobic state at below and above the lower critical solution temperature (LCST) of around 32°C in the aqueous phase.[7] This results in the conversion of the chemical and physical environments among the macromolecule chains and transforms their properties.[8] These environmentally responsive polymer–nanoparticle hybrids facilitate a variety of novel technological applications, such as drug delivery, switchable microfilters, chemical separation, and catalysis.[9] Tenhu and co-workers have shown that the reversible-addition-fragmentation chain-transfer polymerization can produce homogeneous polymer layers on gold nanoparticle surfaces. Such PNIPAM–gold nanocomposites display a low solubility in water because of the low degree of grafting of PNIPAM ligands.[10] Previously, we reported that the thermosensitive copolymer nanotubes of *N*-isopropylacrylamide (NIPAM) and *N*,*N*′-methylenebisacrylamide (MBAA) by ATRP can be fabricated within a porous membrane.[11] The pore size of the copolymer network of PNIPAM-*co*-MBAA can be controlled by the feed ratio of monomers in polymerization. Herein, we report the fabrication of thermosensitive copoly-

[a] Dr. D. Li, Dr. Q. He, Dr. Y. Cui, K. Wang, X. Zhang, Prof. Dr. J. Li
Beijing National Laboratory for Molecular Sciences (BNLMS)
International Joint Lab
CAS Key Lab of Colloid and Interface Science
Institute of Chemistry, Chinese Academy of Sciences
Zhong Guan Cun, Beijing 100080 (P.R. China)
Fax: (+86) 10-8261-2629
E-mail: jbli@iccas.ac.cn

[b] Dr. Q. He
Max Planck Institute of Colloids and Interfaces
14476 Golm/Potsdam (Germany)

mer–gold nanoparticle hybrids and demonstrate their nanocomposite encapsulation by the copolymer network anchored on the gold surface. The slightly cross-linked copolymer chains create a porous nanostructure that is responsive to temperature change. Therefore, such assembled gold nanoparticle–copolymer hybrids (Au@copolymer) can be used to trap and encapsulate other nanoparticles, biomolecules, dyes, or drugs by a temperature-introduced "breathing" process. The whole experimental procedure of Au@copolymer fabrication is illustrated in Scheme 1. The gold

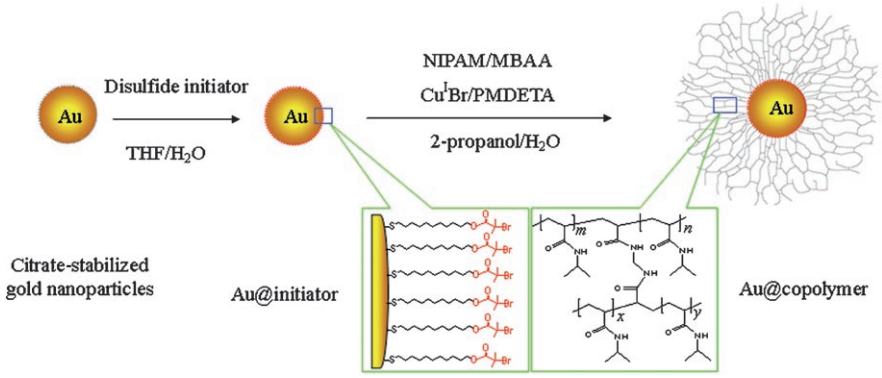

Scheme 1. Au@copolymer fabrication.

nanoparticles were modified by disulfide initiator (Au@initiator) and the ATRP reactions of acrylamide monomers were performed in 2-propanol/water and catalyzed by *N*,*N*,*N*′,*N*′,*N*″-pentamethyldiethylenetriamine (PMDETA) and a $Cu^{I}Br$ catalytic system. The thickness of the polymer shell can be controlled by the concentration of monomers and by the reaction time. The feed ratio of the cross-linker MBAA to NIPAM can influence the network space of the copolymer shell.

Results and discussion

Gold nanoparticles with diameters of 18 nm were synthesized by using the conventional citrate-reduction method.[12] The immobilization of disulfide initiator on the gold surface was achieved through ligand exchange between disulfide and citrate. The Au@initiator nanoparticles obtained are more hydrophobic due to the alkyl chain of the disulfide initiator and can be easily dispersed in THF or DMF without aggregation, as shown in Figure 1A. The elemental analysis of as-prepared samples determined by X-ray photoelectron spectroscopy (XPS) indicates the contributions of O (13.43%), C (58.59%), S (1.65%), Au (26.34%), and a weak signal of Br. Figure 1B shows the detailed binding-energy analysis of C 1s. The four peaks at 284.8, 285.5, 286.7, and 289.6 eV represent the four different carbon atoms marked 1–4, respectively. The peak-fitting result reveals that the atom ratio of C–H/C–C:C–O:C–S/C–Br:C=O is 11:1.09:2.16:0.85, which is consistent with the theoretical value (11:1:2:1) of the pure disulfide initiator. Figure 1C shows the binding-energy increase of Au 4f within a range of 1.3 eV (82.7 to 84.0 eV for Au $4f_{7/2}$ and 86.3 to 87.6 eV for Au $4f_{5/2}$) after (a) and before (b) gold nanoparticle modification by disulfide initiator. This proves the formation of Au–S bonds on the gold surface.[13] The FTIR spectrum of the Au@initiator is similar to that of pure disulfide initiator, as shown in Figure 2. The characteristic absorbance at 2922, 2850 cm^{-1} (CH_2 stretching) and 1735 cm^{-1} (ester carbonyl stretching) further verifies the presence of disulfide initiator molecules.

Next, the surface-initiated ATRP of NIPAM and MBAA monomers with the samples described above was carried out in protic solvents of 2-propanol and water at room temperature. An optimized concentration of NIPAM monomer was 0.4 M and increasing feed ratios of MBAA to NIPAM of 0, 0.5, 1, and 2% were used to change the cross-linking ratio for the comparative studies. The Au@copolymer hybrids obtained were tested in both aqueous and organic solvents and the results show that they have good solubility in both cases. The FTIR spectra of the four samples with different cross-linking ratios are similar, as shown in Figure 2. The main characteristic peak assignments are at 3297 cm^{-1} (secondary amide N–H stretching), 2974 cm^{-1} (CH_3 asymmetric stretching), 1645, and 1552 cm^{-1} (secondary amide C=O stretching),[11] indicating the main contribution of PNIPAM to Au@copolymer hybrids. Notably, the contribution from the cross-linker MBAA in the FTIR spectra may be obscured by that of PNIPAM, as the former is present in a low amount and has a chemical structure similar to NIPAM. The TEM images in Figure 3A show the morphology of linear PNIPAM-modified gold nanoparticles. The core-shell nanoparticles are well dispersed and the polymer shell is clearly visible. With the addition of cross-linker (1% MBAA), the contribution of copolymer shell becomes more obvious, as shown in Figure 3B. The "soft" copolymer layer surrounding the gold nanoparticle (dark core) (Figure 3B, inset), takes up more space. The thickness of the copolymer layer is estimated to be about 46 nm, and that of the linear PNIPAM layer is around 36 nm.

Figure 4A shows the thermosensitive characterization of the assembled Au@copolymer hybrids with different cross-linking ratios. The surface plasmon resonance (SPR) peaks from the UV-visible spectra of Au@copolymer hybrids appear at 533 nm in the presence and absence of cross-linker at room temperature. However, as the temperature increases, the SPR peaks undergo a red shift and an abrupt rise occurs at 32 and 34°C, corresponding to the LCST value

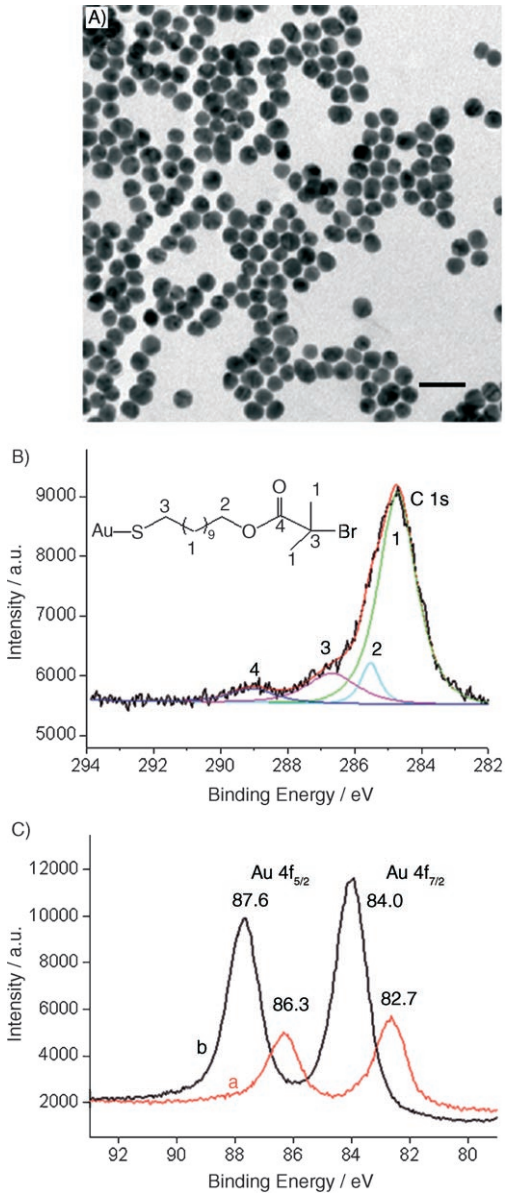

Figure 1. A) TEM image of Au@initiator dispersed in THF. Scale bar: 50 nm. B) C 1s spectra from XPS analysis of Au@initiator. The deconvolution of C 1s: 1 for C–C and C–H, 2 for C–O, 3 for C–S and C–Br, 4 for C=O. C) Au 4f spectra from XPS analysis after (a) and before (b) modification by disulfide initiator.

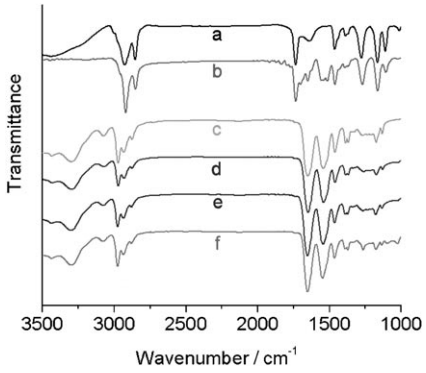

Figure 2. FTIR spectra of a) pure disulfide initiator, b) Au@initiator, and c–f) Au@copolymer hybrids with 0, 0.5, 1, and 2% MBAA, respectively.

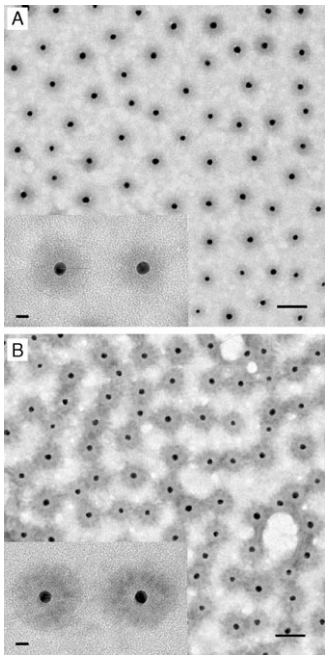

Figure 3. TEM images of Au@copolymer hybrids with A) 0% MBAA and B) 1% MBAA dispersed in water. Scale bars: 100 nm. Insets: images at a higher magnification, scale bars: 20 nm.

of the samples with different feed ratios of cross-linker. A proportion of 0.5% MBAA does not affect the LCST value, however, as the feed ratio increases to 1 or 2%, the LCST value increases to 34°C and, thus, the effect of the cross-linker upon the thermosensitive curves become significant. Moreover, as a visible thermoresponse, the optical color of Au@copolymer hybrids in aqueous suspension also dramatically changes from transparent red to opaque pink as the temperature increases from 25 to 38°C, as shown in Figure 4B. Figure 4C shows the transmittance of the Au@copolymer hybrids in imitating the "breathing" process over ten cycles and reveals almost consistent values. This indicates that the suspension is transparent at 25°C (transmittance of 86%) and opaque at 38°C (transmittance of about 74%). The zigzag curve further demonstrates the reversible thermosensitive response of the Au@copolymer hybrids to temperature changes. Notably, there is no obvious precipitation observed at 38°C. This is because the size of the thermosensitive Au@copolymer hybrids is still on the nanoscale (about 200–300 nm) in aqueous solution, and the temperature change will only alter the thickness of the polymer-coat layer. Thus, no precipitation occurs at high temperature.

The change in size of the Au@copolymer hybrids at different temperatures is proved by the dynamic light-scattering measurements (DLS) obtained at below and above the LCST. The results suggest that the hydrodynamic radius of the Au@copolymer hybrids is about 160 nm at 25°C and

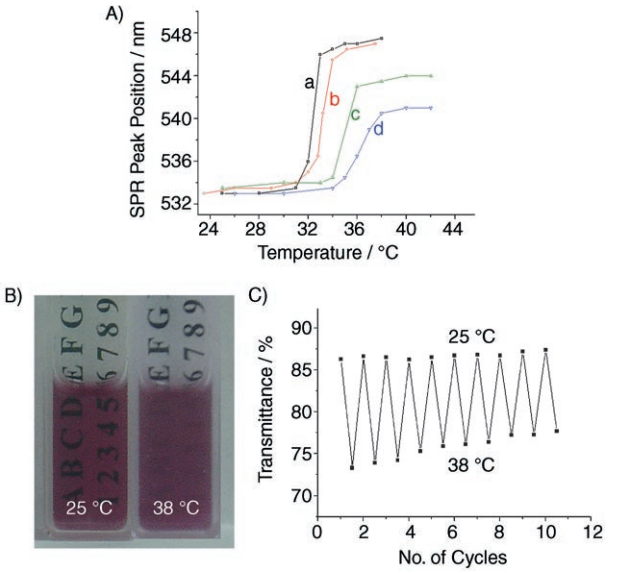

Figure 4. A) Shift in peak position of surface plasmon resonance for Au@copolymer hybrids with a) 0% MBAA, b) 0.5% MBAA, c) 1% MBAA, and d) 2% MBAA. B) Photos of Au@copolymer hybrids with 1% MBAA at 25 and 38°C. C) Reversible transmittance curve of Au@copolymer hybrids with 1% MBAA over ten "breathing" cycles.

112 nm at 38°C. The diameter of these hybrids is clearly large below the LCST and becomes smaller above the LCST. This result also directly reflects the thermosensitive property of the Au@copolymer hybrids. Notably, the size of Au@copolymer hybrids estimated by TEM is obtained by using dried samples. Considering the significant contribution of solvent, the dimensions of the Au@copolymer hybrids obtained in aqueous solution will be larger.

Such assembled Au@copolymer hybrids can be considered to encapsulate small molecules or nanoparticles by virtue of the copolymer-network scaffold. For this purpose, we synthesized 3.5-nm gold nanoparticles to explore the trapping capability of the core-shell nanostructure. We added a dilute solution of the 3.5-nm gold nanoparticles into the suspension of Au@copolymer hybrids (with 1% MBAA) under stirring and incubated the mixture for 30 min in a still state at 25°C and then at 38°C. After repeating this process three times, we obtained the final samples after washing by centrifugation. Figure 5 shows the TEM image of gold nanoparticles encapsulated by the Au@copolymer hybrids. The dark dots located in the "shell" structures indicate the existence of 3.5-nm gold nanoparticles. By comparing this with the TEM image in Figure 3B, we can see that the gold nanoparticles have been trapped within the polymer network and the encapsulated gold nanoparticles are less aggregated. Thus, this procedure can be generalized for the encapsulation of other nanoparticles or larger biomolecules.

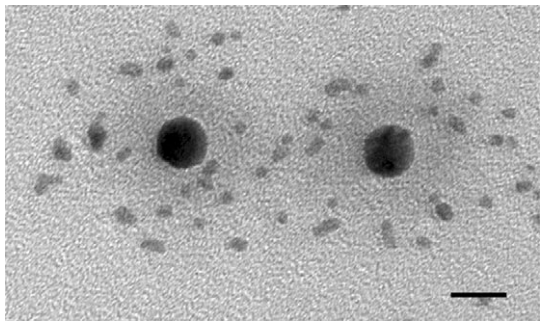

Figure 5. TEM image of Au@copolymer hybrids with 1% MBAA encapsulating 3.5-nm gold nanoparticles. Scale bar: 20 nm.

The thermosensitive mechanism is commonly interpreted as a transformation in the state of the copolymer chains with "expire" and "inspire" water behavior, involving two formation processes of intermolecular and intramolecular hydrogen bonds.[8,11] Below the LCST, the formation of intermolecular hydrogen bonds promotes absorption of a quantity of water, causing the polymer chains to swell; the so-called "inspire" water process. Above the LCST, the formation of intramolecular hydrogen bonds will exclude the polymer-bonded water, causing the polymer chains to shrink to the gold cores, forcing the water molecules out of the polymer space; the "expire" water process. The alternative "inspiration" and "expiration" of water imitates the "breathing" process, as illustrated in Scheme 2. Thus, the breathing process of the polymer shell as the temperature changes promotes the flow of water molecules into and out of the polymer network. This so-formed water flow takes gold nanoparticles into the polymer network, accompanied by the effect of diffusion.

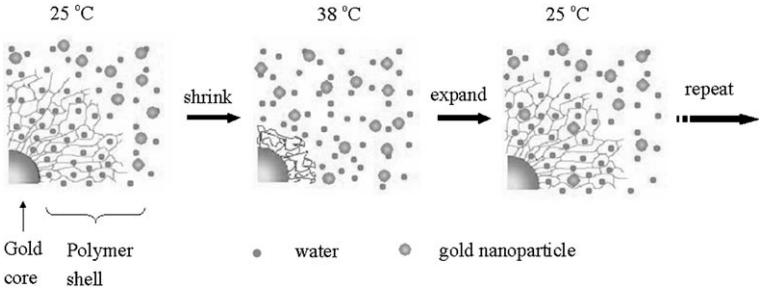

Scheme 2. The "breathing" mechanism and encapsulation process.

Conclusions

We have demonstrated that the disulfide initiator can be successfully immobilized onto the surface of gold nanoparticles to initiate the ATRP of acrylamide monomers under ambient conditions to construct Au@copolymer hybrids. These Au@copolymer hybrids have a distinct core-shell

structure and good dispersity in both the aqueous and organic phases. The copolymer "shell" has a network scaffold that is clearly thermosensitive and that can trap nanoparticles by using the "breathing" mechanism. Such assembled Au@copolymer hybrids provide a means to potential uses in delivery biomolecules, catalysts, and drugs.

Experimental Section

Materials: 11-Mercapto-1-undecanol, 2-bromo-2-methylpropionyl bromide, *N*-isopropylacrylamide (NIPAM), and *N*,*N*,*N*′,*N*′,*N*″-pentamethyldiethylenetriamine (PMDETA) were purchased from Aldrich. *N*,*N*′-methylenebisacrylamide (MBAA) and $Cu^{I}Br$ were obtained from the Beijing Chemical Reagent Corp., China. Gold nanoparticles of average sizes 18 and 3.5 nm were prepared with 0.24 mM $HAuCl_4$ by using the citrate-reduction method and the $NaBH_4$-reduction method, respectively.[12] The disulfide initiator $[S\text{-}(CH_2)_{11}\text{-}OCOC(CH_3)_2Br]_2$ for ATRP was synthesized from 11-mercapto-1-undecanol and 2-bromo-2-methylpropionyl bromide by using a modified procedure according to reference [14] and was characterized by ^1H and ^{13}C NMR spectroscopy and by elemental analysis.

Preparation of Au@initiator: The disulfide initiator was immobilized on the surface of gold nanoparticles by ligand exchange with citrate. A certain volume of the 18-nm gold nanoparticle suspension was slowly added to the same volume of disulfide initiator solution (3.0 mM) in THF with stirring for 24 h. Then the Au@initiator samples were collected and washed with THF, 2-propanol, and deionized water by centrifugation. The final samples were dispersed in THF and were stored at −20°C.

Preparation of Au@copolymer hybrids by ATRP: Growth of polymer chains on the surface of gold nanoparticles was performed at RT, referring to our previous work.[11] Briefly, Au@initiator (about 2 mg), NIPAM (0.905 g, 8 mmol), $Cu^{I}Br$ (14.3 mg, 0.1 mmol), and a certain amount of MBAA (0, 6.5, 12.5, or 25 mg, corresponding to a 0, 0.5, 1, or 2% feed ratio of MBAA to NIPAM, respectively) were added to a round-bottomed flask and the mixture was degassed by three freeze-pump-thaw cycles with N_2. A degassed solution of PMDETA (52.0 mg, 0.3 mmol) dissolved in 2-propanol/water (1:1, 2 mL) was injected into the flask with vigorous stirring. The reaction was performed for 3 h and was terminated by opening the system to air. The as-prepared hybrids were purified by repeating the cycles of centrifugation, 2-propaol/water wash, and redispersion. Finally, the sample hybrids were dispersed in water.

Thermosensitivity of Au@copolymer hybrids: UV/Vis spectra of Au@copolymer hybrid suspensions of about 0.5 nM containing different feed ratios of MBAA were recorded at different temperatures to analyze the thermosensitive response of the SPR of gold nanoparticles. The transmittance change of the Au@copolymer hybrids was then detected at a wavelength of 740 nm by using a UV/Vis spectrometer after the sample was kept at 25 and 38°C for 30 min, respectively. This procedure was repeated ten times.

Encapsulation experiments: A solution of Au@copolymer hybrids (about 0.5 nM with 1% MBAA) and a dilute solution of 3.5-nm gold nanoparticles were mixed under stirring. The mixture was incubated in a still state for 30 min at 25°C, then at 38°C, respectively, and this was repeated three times. The excess gold nanoparticles were washed out by centrifugation at low temperature.

Instrumentation: FTIR and UV/Vis spectra were recorded by using a TENSOR 27 instrument (BRUKER) and a U-3010 UV/Vis spectrometer (HITACHI), respectively. X-ray photoelectron spectroscopy (XPS) was performed by using a ESCALab220i-XL (VG Scientific). TEM images of various nanoparticles were obtained by using a TECNAI 20 transition electronic microscope (PHILIPS). The Au@copolymer samples were stained for TEM observation on copper grids by using 0.5% phosphotungstic acid.

Acknowledgements

We acknowledge the financial supports of this research by the National Nature Science Foundation of China (No. 20404015 and 90206035) as well as the collaborated project of the German Max-Plank Society.

[1] a) M. Brust, M. Walker, D. Bethell, D. J. Schiffrin, R. Whyman, *J. Chem. Soc. Chem. Commun.* **1994**, 801–802; b) M. J. Hostetler, J. E. Wingate, C. J. Zhong, J. E. Harris, R. W. Vachet, M. R. Clark, J. D. Londono, S. J. Green, J. J. Stokes, G. D. Wignall, G. L. Glish, M. D. Porter, N. D. Evans, R. W. Murray, *Langmuir* **1998**, *14*, 17–30; c) X. Zhao, X. Ding, Z. Deng, Z. Zheng, Y. Peng, X. Long, *Macromol. Rapid Commun.* **2005**, *26*, 1784–1787; d) W. P. McConnell, J. P. Novak, L. C. Brousseau III, R. R. Fuierer, R. C. Tenent, D. L. Feldheim, *J. Phys. Chem. B* **2000**, *104*, 8925–8930.

[2] a) C. M. Niemeyer, *Angew. Chem.* **2001**, *113*, 4254–4287; *Angew. Chem. Int. Ed.* **2001**, *40*, 4128–4158; b) N. Levit-Binnun, A. B. Lindner, O. Zik, Z. Eshhar, E. Moses, *Anal. Chem.* **2003**, *75*, 1436–1441; c) Y. Xiao, F. Patolsky, E. Katz, J. F. Hainfeld, I. Willner, *Science* **2003**, *299*, 1877–1881; d) C. M. Niemeyer, *Angew. Chem.* **2003**, *115*, 5974–5978; *Angew. Chem. Int. Ed.* **2003**, *42*, 5796–5800.

[3] a) W. P. Wuelfing, S. M. Gross, D. T. Miles, R. W. Murray, *J. Am. Chem. Soc.* **1998**, *120*, 12696–12697; b) T. Teranishi, I. Kiyokawa, M. Miyake, *Adv. Mater.* **1998**, *10*, 596–599; c) A. B. Lowe, B. S. Sumerlin, M. S. Donovan, C. L. McCormick, *J. Am. Chem. Soc.* **2002**, *124*, 11562–11563; d) C. Mangeney, F. Ferrage, I. Aujard, V. Marchi-Artzner, L. Jullien, O. Ouari, E. D. Rekai, A. Laschewsky, I. Vikholm, J. W. Sadowski, *J. Am. Chem. Soc.* **2002**, *124*, 5811–5821.

[4] R. Jordan, N. West, A. Ulman, Y. Chou, O. Nuyken, *Macromolecules* **2001**, *34*, 1606–1611.

[5] K. J. Watson, J. Zhu, S. T. Nguyen, C. A. Mirkin, *J. Am. Chem. Soc.* **1999**, *121*, 462–463.

[6] a) T. E. Patten, K. Matyjaszewski, *Adv. Mater.* **1998**, *10*, 901–915; b) S. Nuß, H. Böttcher, H. Wurm, M. L. Hallensleben, *Angew. Chem.* **2001**, *113*, 4137–4139; *Angew. Chem. Int. Ed.* **2001**, *40*, 4016–4018; c) K. Ohno, K. Koh, Y. Tsujii, T. Fukuda, *Macromolecules* **2002**, *35*, 8989–8993; d) T. K. Mandal, M. S. Fleming, D. R. Walt. , *Nano Lett.* **2002**, *2*, 3–7; e) H. Duan, M. Kuang, G. Zhang, D. Wang, D. G. Kurth, H. Möhwald, *Langmuir* **2005**, *21*, 11495–11499; f) Y. Lu, Y. Mei, M. Drechsler, M. Ballauff, *Angew. Chem.* **2006**, *118*, 827–830; *Angew. Chem. Int. Ed.* **2006**, *45*, 813–816.

[7] a) R. H. Pelton, H. M. Pelton, A. Morphesis, R. L. Rowell, *Langmuir* **1989**, *5*, 816–818; b) H. G. Schild, D. A. Tirrell, *J. Phys. Chem.* **1990**, *94*, 4352–4356.

[8] a) E. C. Cho, J. Lee, K. Cho, *Macromolecules* **2003**, *36*, 9929–9934; b) Z. Hu, X. Xia, *Adv. Mater.* **2004**, *16*, 305–309; c) D. Gan, L. A. Lyon, *J. Am. Chem. Soc.* **2001**, *123*, 8203–8209; d) N. C. Woodward, B. Z. Chowdhry, M. J. Snowden, S. A. Leharne, P. C. Griffiths, A. L. Winnington, *Langmuir* **2003**, *19*, 3202–3211; e) T. J. V. Prazeres, A. M. Santos, J. M. G. Martinho, A. Elaissari, C. Pichot, *Langmuir* **2004**, *20*, 6834–6840; f) T. Hellweg, C. D. Dewhurst, W. Eimer, K. Kratz, *Langmuir* **2004**, *20*, 4330–4335.

[9] a) D. E. Bergbreiter, B. L. Case, Y. S. Liu, J. W. Caraway, *Macromolecules* **1998**, *31*, 6053–6062; b) J. H. Kim, T. R. Lee, *Chem. Mater.* **2004**, *16*, 3647–3651; c) C. Li, N. Gunari, K. Fischer, A. Janshoff, M. Schmidt, *Angew. Chem.* **2004**, *116*, 1121–1124; *Angew. Chem. Int. Ed.* **2004**, *43*, 1101–1104; d) C. M. Schilli, M. Zhang, E. Rizzardo, S. H. Thang, Y. K. Chong, K. Edwards, G. Karlsson, A. H. E. Muller, *Macromolecules* **2004**, *37*, 7861–7866; e) S. Liu, Y. Yang, X. Liu, Y. Tong, *Biomacromolecules* **2003**, *4*, 1784–1793; f) D. Kim, J. Heo, K. Kim, I. Choi, *Macromol. Rapid Commun.* **2003**, *24*, 517–521; g) G. V. Rama Rao, M. E. Krug, S. Balamurugan, H. Xu, Q. Xu, G. P. Lopez, *Chem. Mater.* **2002**, *14*, 5075–5080; h) H. Kanazawa, Y. Kashiwase, K. Yamamoto, Y. Matsushima, A. Kikuchi, Y. Sakurai, T. Okano, *Anal. Chem.* **1997**, *69*, 823–830.

[10] J. Raula, J. Shan, M. Nuopponen, A. Niskanen, H. Jiang, E. I. Kauppinen, H. Tenhu, *Langmuir* **2003**, *19*, 3499–3504.

[11] Y. Cui, C. Tao, S. Zheng, Q. He, S. Ai, J. Li, *Macromol. Rapid Commun.* **2005**, *26*, 1552–1556.
[12] a) S. Link, M. A. El-Sayed, *J. Phys. Chem. B* **1999**, *103*, 8410–8426; b) K. Aslan, C. C. Luhrs, V. H. Perez-Luna, *J. Phys. Chem. B* **2004**, *108*, 15631–15639; c) N. R. Jana, L. Gearheart, C. J. Murphy, *Langmuir* **2001**, *17*, 6782–6786.
[13] E. C. Cho, Y. D. Kim, K. Cho, *Polymer* **2004**, *45*, 3195–3204.
[14] R. R. Shah, D. Merreceyes, M. Husemann, I. Rees, N. L. Abbott, C. J. Hawker, J. L. Hedrick, *Macromolecules* **2000**, *33*, 597–605.

Received: July 27, 2006
Published online: December 11, 2006

